

Published in final edited form as:

Inorg Chem. 2010 December 6; 49(23): 11030–11038. doi:10.1021/ic101515g.

The Bis(μ -oxo) Dicopper(III) Species of the Simplest Peralkylated Diamine: Enhanced Reactivity towards Exogenous Substrates

 Peng Kang^[a], Elena Bobyr^[a], John Dustman^[a], Keith O. Hodgson^{[a],[b],*}, Britt Hedman^{[b],*}, Edward I. Solomon^{[a],[b],*}, and T. Daniel P. Stack^{[a],*}
^[a] Department of Chemistry, Stanford University, Stanford, California 94305

^[b] Stanford Synchrotron Radiation Lightsource, SLAC, Stanford University, Menlo Park, California 94025

Abstract

N,N,N',N'-tetramethylethylenediamine (TMED), the simplest and most extensively used peralkylated diamine ligand, is conspicuously absent from those known to form a bis(μ -oxo)dicopper(III) (**O**) species, [(TMED)₂Cu(III)₂O₂]²⁺, upon oxygenation of its Cu(I) complex. Presented here is the characterization of this **O** species and its reactivity towards exogenous substrates. Its formation is complicated both by the instability of the [(TMED)Cu(I)]¹⁺ precursor and by competitive formation of a presumed mixed-valent trinuclear [(TMED)₃Cu₃(μ_3 -O)₂]³⁺ (**T**) species. Under most reaction conditions, the **T** species dominates, yet, the **O** species can be formed preferentially (> 80%) upon oxygenation of acetone solutions, if the copper concentration is low (< 2 mM) and [(TMED)Cu(I)]¹⁺ is prepared immediately before use. The experimental data of this simplest **O** species provides a benchmark by which to evaluate DFT computational methods for geometry optimization and spectroscopic predictions. The enhanced thermal stability of [(TMED)₂Cu(III)₂O₂]²⁺ and its limited steric demands compared to other **O** species allows more efficient oxidation of exogenous substrates, including benzyl alcohol to benzaldehyde (80% yield), highlighting the importance of ligand structure to not only enhance the oxidant stability but also maintain accessibility to the nascent metal/O₂ oxidant.

1. Introduction

Bis(μ -oxo)dicopper(III) (**O**) species have attracted considerable interests in the past decade^{1–5} as a high-valent metal-oxo species that is formed by the reaction of a wide variety of Cu(I) complexes with dioxygen (O₂). Though unknown until the mid-1990s, the **O** species is now the most characterized all Cu-O₂ products and can exist in a facile equilibrium with appreciable amounts of the isomeric μ - η^2 : η^2 -peroxodicopper(II) (**SP**) species,^{6–8} the characterized oxygenated species of tyrosinase (Tyr), catechol oxidase and hemocyanin.⁹ Given the close structural and energetic relationship of **O** and **SP** isomers, the nature of the active oxidant in tyrosinase is an open issue considering that several synthetic systems stabilizing a spectroscopically and structurally faithful **SP** mimic of oxy-Tyr are

hodgson@ssrl.slac.stanford.edu; hedman@ssrl.slac.stanford.edu; edward.solomon@stanford.edu; stack@stanford.edu.

 Supporting Information Available: Full reference of Gaussian 03, titration of the TMED **O** species with FcCOOH, X-ray absorption spectroscopy of the **O** species with CF₃SO₃[−] and SbF₆[−], Eyring plot of the TMED **O** species, Cartesian coordinates of optimized D₂ conformation of the TMED **O** species and Mulliken population analysis of selected molecular orbitals. This material is available free of charge via the Internet at <http://pubs.acs.org>.

capable of hydroxylating exogenously added phenolates to catecholates through the immediacy of an **O** type species.¹⁰

Numerous nitrogen-based ligands have been systematically explored for their ability to stabilize **O** species,¹ such as alkyl amines,^{11,12} pyridines,¹³ diketiminates¹⁴ and most recently guanidines¹⁵ at low temperatures (193 K) with weakly coordinating anions in non-protic solvents. The ligand attributes that correlated with **O** formation are electron-rich bidentate ligands capable of stabilizing a d⁸ Cu(III) center and sufficient steric demands to preclude the formation of a nonreactive [(L)₂Cu(I)]¹⁺ complex. Tridentate and tetradentate mononucleating, nitrogen-based ligands can stabilize the **O** species, albeit this occurs by a denticity reduction, in which a ligating atom does not associate closely with the copper center.¹ The steric demands of the described bidentate ligands tend to stabilize three-coordinate Cu(I) complexes in which the third ligand is derived from a weakly associated anion or solvent molecule such as acetonitrile. While such complexes provide access of O₂ to the copper center and rapid formation of the **O** species, this dimer is very compact with a Cu...Cu distance of only 2.73–2.85 Å. The consequence is that neither the copper centers nor the oxide ligands are very accessible to exogenous substrates. Predictably, the larger the steric demands, the more oxidative damage that is inflicted on the ligand upon warming these **O** species to ambient conditions. Intramolecular ligand hydroxylation is a prevalent decomposition pathway,¹⁶ thereby limiting the thermal stability of most **O** species. Directing this oxidative reactivity outward to exogenous substrates requires minimizing the steric demands of the ligands while retaining oxidatively robust substituents.

We have extensively explored the peralkylated diamine ligands (PDLs) in stabilizing **O** species as simple and versatile ligands (Scheme 1). Systematic variation of the steric demands and bite-angle provides an exquisite probe into the nature of the Cu/O₂ species formed.¹² The three most extensively explored families of PDLs, defined by their parent diamine backbone, are the (*R,R*)-1,2-cyclohexanediamines (CD),¹⁷ 1,2-ethylenediamines (ED)^{8,18} and 1,3-propanediamines (PD).^{19,20} Notably in the ED series, simply reducing the steric demands of alkyl moieties, the predominant Cu/O₂ species shifts from a **SP** species¹⁸ to an **O** species^{17,21} finally to a trinuclear species, [Cu(II,II,III)₃(μ₃-O)₂]³⁺ (**T**),¹² demonstrating the versatility of ED ligands. The aliphatic substituents created strongly basic, tertiary N-donors, which are able to stabilize the high Cu(III) oxidation state at distances longer than secondary amines.

N,N,N',N'-tetramethylethylenediamine (TMED) is the most widely used PDL in Cu-catalyzed aerobic organic transformations.^{22–24} CuCl/amine/O₂ combinations catalytically convert alcohols to aldehydes in high yields under ambient conditions while TMED is among the commonly employed amines. CuCl/TMED/O₂ also oxidatively couples 2,6-disubstituted phenols to form poly-2,6-disubstituted 1,4-phenylene ethers, 2,4-disubstituted phenols to bis-phenols,²⁵ and acetylenes to diacetylenes in high yields.²⁶ However, little information is known about the active Cu/O₂ species that form with TMED and allow the reactions to be catalytic.

As the simplest PDL, TMED stands as a promising ligand to stabilize an accessible **O** species for exogenous substrates and the C–H groups of the methyl substituents should be the most oxidatively robust based on simple bond dissociation energies.¹⁷ However, the expected **O** species by TMED is conspicuously absent from previous studies due to ambiguous and ill-defined oxygenation chemistry.¹² This study discusses the challenges and strategies to stabilize the **O** species formed with TMED and investigates its physical properties and reactivities towards exogenous substrates.

2. Results

Synthesis of (TMED)Cu(I) Complex

[(TMED)Cu(I)]¹⁺ was synthesized by mixing equimolar amounts of TMED and [Cu(I)(MeCN)₄](X) (X⁻ = SbF₆⁻, CF₃SO₃⁻) in dry CH₂Cl₂. Slight deviations from the 1:1 Cu(I):TMED ratio often lead to an unstable [(TMED)Cu(I)]¹⁺ complex or incomplete oxygenation as assessed by optical absorptions. The [(TMED)Cu(I)]¹⁺ solutions degrade faster compared to other PDL-Cu(I) complexes in a N₂ drybox; a yellow precipitate forms within 12 hrs, and over longer periods the solution turns blue accompanied with a brown precipitate presumably due to the disproportionation of the Cu(I) complex. Purification of the Cu(I) complex by a reported method²⁷ yields a white solid, which can be oxygenated at low temperature. However, it still turns into a yellow solid over 24 hrs, which no longer reacts with dioxygen at low temperature. The ligating acetonitrile present in the white solid is lost in the yellow solid by ¹H-NMR analysis, leading to a nonreactive Cu(I) complex towards O₂. The instability of the Cu(I) complex mandates that the Cu(I) solutions are prepared immediately before oxygenation at low temperature for reproducible results.

Oxygenation of [(TMED)Cu(I)]¹⁺ Complex

[(TMED)Cu(I)](X) (X⁻ = SbF₆⁻, CF₃SO₃⁻) solutions were oxygenated by injection into a rapidly stirred O₂-saturated acetone solution at 183 K. The rapid full formation (< 5 sec) of the **O** species is indicated by the yellow color of the initial colorless solution. The 392 nm ligand to metal charge transfer (LMCT) band (Figure 1, ε = 18.5 mM⁻¹ cm⁻¹ per dimer) is consistent with other related **O** species.¹ The intensity of this optical feature is not altered by purging the solution with N₂ nor by evacuating the reaction vessel, consistent with an irreversible oxygenation reaction. Titration of the **O** species with ferrocene monocarboxylic acid, a technique developed to quantify the formation of such oxidizing species,¹⁵ gives 80% of the expected yield calibrated against well-established, fully-formed **O** species (Figure S1).²⁸

This **O** species of TMED only forms in acetone at Cu concentrations less than 2 mM. At higher concentrations (> 10 mM), oxygenation yields a purple solution with a dramatically different optical spectrum, presumably a 3:1 Cu:O₂ trinuclear (**T**) species (Figure 1). The most intense LMCT band of the **T** species occurs at higher energy (345 nm, ε = 12.5 mM⁻¹ cm⁻¹ per trimer) along with two lesser intense bands in the visible spectra (500 nm, ε = 1.3 mM⁻¹ cm⁻¹; 620 nm, ε = 0.9 mM⁻¹ cm⁻¹ per trimer). The energies and extinction coefficients of these three optical features are similar to other reported **T** species with *N,N'*-diethyl-*N,N'*-dimethylethylenediamine (MEED),¹² *N,N,N',N'*-(*R,R*)-1,2-cyclohexanediamine (TMCD)²⁹ and *N,N*-dimethyl-2-(2-pyridyl)ethylamine (^HPy1^{Me,Me}).³⁰ Once the **T** species or the **O** species is formed, no measurable equilibrium between the two species could be detected optically by varying the temperature (183–233 K) or by removing excess O₂.

Resonance Raman Spectroscopy

The resonance Raman spectrum was obtained by excitation into the 392 nm LMCT band at 413 nm (Figure 2). The characteristic symmetric Cu₂O₂ bis-μ-oxo breathing mode of the **O** species occurs at 607 cm⁻¹, shifting by 27 cm⁻¹ to 580 cm⁻¹ upon ¹⁸O₂ substitution.³¹ The peak at 514 cm⁻¹ is presumably a Cu–N stretching mode, which is not sensitive to ¹⁸O₂ isotope substitution. The feature at 1127 cm⁻¹, which shifts by 27 cm⁻¹ with ¹⁸O₂ substitution, is consistent with a combination mode of the symmetric core breathing mode at 607 cm⁻¹ and the Cu–N stretching mode at 514 cm⁻¹. The peak at 1030 cm⁻¹ is presumably an overtone of the Cu–N stretching mode at 514 cm⁻¹, and the peaks at 762 and 950 cm⁻¹ are unassigned ligand stretching modes.

X-ray Absorption Spectroscopy

Cu K-edge X-ray absorption spectroscopy (XAS) was used to probe the oxidation state of Cu and structural parameters of the **O** species. The XAS data with an SbF_6^- anion in acetone (5% CH_2Cl_2 , 1 mM Cu) are most consistent with an **O** species. The X-ray absorption edge displays a $1s \rightarrow 3d$ pre-edge feature at $\sim 8980.3 \pm 0.2$ eV (Figure 3). This value is close to the range of pre-edge values of previously characterized Cu(III) complexes ($\sim 8981.0 \pm 0.5$ eV) and is higher than the pre-edge energy for Cu(II) complexes ($\sim 8979.0 \pm 0.5$ eV).³² Similarly, the pre-edge peak of a closely related **O** complex, $[(\text{TMPD})_2\text{Cu(III)}_2\text{O}_2]^{2+}$ (TMPD = *N,N,N',N'*-tetramethyl-1,3-propanediamine), occurs at ~ 8980.5 eV, an energy value at the lower end of the range expected for a Cu(III) species.¹⁹ The edge exhibits an intense absorption at ~ 8987.3 eV (Figure 3) that is assigned as a $1s \rightarrow 4p$ + shakedown transition for Cu(II) and Cu(III) complexes and is significantly more pronounced for Cu(III) than for Cu(II).³² The EXAFS data are fitted adequately with a model consisting of 2 O at 1.80 Å ($\sigma^2 = 0.0038$ Å²), 2 N at 1.96 Å ($\sigma^2 = 0.0041$ Å²), 1 Cu at 2.74 Å ($\sigma^2 = 0.0026$ Å²) and 6 C at 2.77 Å ($\sigma^2 = 0.0207$ Å²) (Figure 4). The short Cu–O and Cu–Cu distances are characteristic of an **O** core, which typically exhibit a Cu–O bond length of 1.79–1.86 Å and a Cu··Cu separation of 2.74–2.91 Å.¹ Identical structural parameters were obtained for the **O** species with the CF_3SO_3^- and SbF_6^- counteranions (Figure S2 and Table S1),²⁸ suggesting that neither anion closely associates with the Cu_2O_2 core.

Thermal Decomposition

Thermal decomposition kinetics and the decomposition product were examined to elucidate the thermal decomposition mechanism of this **O** species. The decay of the **O** species, initially formed in acetone at 183 K and rapidly warmed to an appropriate temperature, was monitored by the disappearance of the 392 nm UV-Vis feature. The decay was recorded at various temperatures (256–279 K), and the time-dependent spectra (320–600 nm) at each temperature were fitted by multi-wavelength analysis as simple first order A→B process. An Eyring analysis (Figure S3)²⁸ gave a $\Delta H^\ddagger = 15(1)$ kcal mol⁻¹ and $\Delta S^\ddagger = -15(2)$ cal K⁻¹ mol⁻¹. The ligand products recovered after a basic work-up were *ca.* 75% intact ligand and 25% mono-demethylated ligand as assessed by GC and GC-MS analysis, accounting for a 50% yield in ligand N-dealkylation assuming the **O** species as a 2-electron oxidant.

Reactivity with Exogenous Substrates

$[(\text{TMED})_2\text{Cu(III)}_2\text{O}_2]^{2+}$ stoichiometrically oxidizes benzyl alcohol and phenolic substrates at 243 K. Two equivalents of alcohol or phenol substrates were added to the **O** species after the removal of excess O_2 by multiple cycles of purging and evacuation, and the decay kinetics of the **O** species were monitored at 392 nm until this optical feature was fully quenched each time. After an aqueous workup, the organic products were quantified by GC and/or GC-MS for benzyl alcohol and by ¹H-NMR for the phenolic substrates. Assuming that the **O** species serves as a 2-electron oxidant, benzyl alcohol is oxidized to benzaldehyde in *ca.* 80% yield relative to the **O** species, whereas octanol does not react. 2,4-Di-*tert*-butylphenol is coupled to 3,3',5,5'-tetra-*tert*-butyl-2,2'-bisphenol in a 40% yield, comparable to that of other PDL **O** species, consistent with a *ca.* 50% maximum yield measured from other **O** species with excess O_2 fully removed.^{15,33}

The mechanism of benzyl alcohol oxidation was further probed using various deuterated benzyl alcohols both by competitive and absolute measurements of the rate of decay of $[(\text{TMED})_2\text{Cu(III)}_2\text{O}_2]^{2+}$ species. The intramolecular competition experiment of the oxidation of *α*-*d*₁-benzyl alcohol gave a 2.8(1):1 *α*-*d*₁-benzaldehyde/*α*-*h*₁-benzaldehyde ratio (GC-MS analysis), indicating clearly that *α*C–H(D) bond cleavage occurs in the product determining step of the reaction (Table 1). The intermolecular competition experiments with a 1:1 mixture of *α,α*-*h*₂ and *α,α*-*d*₂ benzyl alcohol by product analysis are consistent with the

intra-molecular results, yielding a 3.5(2):1 ratio of α - h_1 -benzaldehyde/ α - d_1 -benzaldehyde.³⁴ The absolute rate of the oxidation of α , α - h_2 and α , α - d_2 benzyl alcohol were measured independently at 243 K by monitoring the decay of the 392 nm **O** feature using a 20-fold excess of substrate. Under these conditions, a pseudo first-order decay was measured for each substrate yielding a KIE value (k_h/k_d) of 3.3(4). The comparable competitive and absolute kinetic isotope effects are consistent with a single rate and product determining step involving C–H bond cleavage. Deuteration of the hydroxyl proton on benzyl alcohol only slightly impacted the oxidation rate (KIE = 1.12(7), Table 1).

DFT Computations

The geometry of [(TMED)₂Cu(III)₂O₂]²⁺ is optimized by density functional theory (DFT) calculations, which is significantly more stable than the ⁵P isomer (vacuum, electronic energies: 7.8 kcal mol⁻¹ at B3LYP/BS1//B3LYP/6-31G(d),³⁵ 15.1 kcal mol⁻¹ at BLYP/BS1//B3LYP/6-31G(d)). The optimized metrical parameters of TMED **O** species are variable depending upon the functional and basis set used (Table 2). In all cases, no core potentials were used for the copper centers, as such basis sets lead to expanded Cu₂O₂N₄ cores relative to known experimental metrical values. An increase in the Hartree-Fock (HF) percentage in the functional (from 0% in BLYP to 50% in BHandHLYP) or a reduction in the size of basis set (from BS1 to 6-31G(d)) generally leads to shorter Cu...Cu and Cu–O distances. The B3LYP/6-31G(d) optimized structure (Figure 5a) provides the closest agreement with the metrical parameters from the experimental-derived EXAFS model. The two limiting, high-symmetry conformations (*D*₂ and *C*_{2h}; Figure 5b) exist for [(TMED)₂Cu(III)₂O₂]²⁺ due to the relative twisting of the 5-membered chelate rings of the ligands. The optimized *D*₂ structure is *ca.* 0.3 kcal mol⁻¹ lower in energy with the energy evaluated at a B3LYP/BS1 level of theory (B3LYP/BS1//B3LYP/6-31G(d)). All subsequent computations used this *D*₂ optimized geometry. The non-scaled³⁶ computed Raman spectrum predicts an intense A₁ Cu₂O₂ breathing mode at 679 cm⁻¹ that shifts to 647 cm⁻¹ ($\Delta = 32$ cm⁻¹) upon ¹⁸O₂ substitution (Table 3). This compares qualitatively with the 607 cm⁻¹ experimental resonance Raman feature of the Cu₂O₂ core mode ($\lambda_{\text{ex}} = 413$ nm) that shifts to 580 cm⁻¹ ($\Delta = 27$ cm⁻¹) upon ¹⁸O₂ substitution. The vibration calculation also predicts an intense A₁ symmetric Cu₂O₂ vibration mode at 141 cm⁻¹ that is ¹⁸O isotope insensitive in agreement with experimental values for other simple **O** species formed with PDLs (*ca.* 120–135 cm⁻¹).³¹

Theoretical electronic spectra were calculated using time-dependent DFT (TD-DFT) with various methods (Table 4). Increasing the percentage of HF in the functional or reducing the basis set size results in a blue-shift of the *ca.* 390 nm LMCT band. While a PCM solvation model only marginally shifts the energy of this feature compared with vacuum, the relative oscillator strengths of the 390 nm band with another predicted *ca.* 290 nm LMCT band are much more balanced, consistent with other **O** species investigated in solvents that allow both bands to be measured.¹ A simulated spectrum using the experimental bandwidth of the 392 nm feature (Figure 6) shows a LMCT at 357 nm ($\epsilon = 30$ mM⁻¹ cm⁻¹) compared to the 392 nm ($\epsilon_{\text{corr}} = 23$ mM⁻¹ cm⁻¹)³⁷ experimental value. Population analysis (Table S2)²⁸ suggests that this LMCT band is composed partially of a dioxo σ^* orbital (HOMO-1) to Cu d_{xy} orbital (LUMO+1) transition, consistent with previous assignments in the literature.³¹ Another intense LMCT band is predicted at *ca.* 290 nm; population analysis supports a dioxo π_{σ}^* orbital (HOMO-5) to Cu d_{xy} orbital (LUMO) transition. This feature is not observed experimentally due to acetone absorption in this region.

3. Discussion

Formation of O Species

A diverse array of thermally sensitive species are formed in the reaction of Cu(I) complexes with O₂. The formation and stabilization of such species depends on ligand, concentration of Cu, solvent, counteranion and temperature.¹ With Cu(I) complexes that react with O₂, the steric demands of the ligand predominately determines the type of Cu/O₂ species that forms with the ligand electronics, solvent, counteranions and temperature playing an important but subordinate role. In the present study, the limited ligand steric demands of *N,N,N',N'*-tetramethylethylenediamine (TMED) in [(TMED)Cu(I)]¹⁺ very much complicates its oxygenation reaction as two spectroscopically distinct, thermally sensitive Cu-O₂ species are formed with a 2:1 and 3:1 Cu:O₂ stoichiometry. The former is characterized in this study as [(TMED)₂Cu(III)O₂]²⁺ complex, an **O** species, and the latter is postulated as a trinuclear [(TMED)₃Cu(III)Cu(II)O₂]³⁺ complex, a **T** species. Additional complications in the oxygenation reaction result from the limited stability of [(TMED)Cu(I)]¹⁺ with weakly coordinating anions in aprotic, dry solvents, even under an inert atmosphere. Peralkylated diamine (PDL) Cu(I) complexes generally ligate one or two, acetonitrile ligands, creating either a trigonal or tetrahedral complex, respectively. Acetonitrile loss and anion association to the copper center often leads to degradation or oligomerization of the complexes, which is especially prominent in less steric PDLs such as TMED with more exposed copper center. In this case, the resulted yellow precipitate does not oxygenate to a detectable, thermal-sensitive species under our standard conditions. Degradation of a rapidly precipitated white solid of [(TMED)Cu(I)]¹⁺ even occurs in the solid state under a dinitrogen atmosphere at room temperature (RT). The least sterically demanding ligands such as TMED can also form a colorless 2:1 complex, [(TMED)₂Cu(I)]¹⁺, that has been structurally characterized³⁸ and also does not readily oxygenate.

These complications clearly explain the dearth of data on the oxygenated forms of [(TMED)Cu(I)]¹⁺ complex with the simplest of the peralkylated diamine ligand, especially considering that perethylated variant, *N,N,N',N'*-tetraethylethylenediamine (TEED), forms an isolable Cu(I) complex that oxygenates cleanly to an **O** species. Yet, the simplicity of TMED warrants an investigation of the oxygenation of [(TMED)Cu(I)]¹⁺ if only to determine the reactivity of the **O** species in its most sterically unencumbered form. The conditions that best stabilize in situ prepared [(TMED)Cu(I)]¹⁺ use weakly coordinating anions such as SbF₆⁻ and CF₃SO₃⁻ in dry CH₂Cl₂. Much faster degradation occurs with the more coordinating CH₃SO₃⁻ anion even in dry CH₂Cl₂. Even given the optimized conditions for stabilizing [(TMED)Cu(I)]¹⁺, the most reproducible oxygenation results were collected from freshly prepared solutions and then only at an 80% yield.

A second challenge in maximizing the formation of the **O** species is the competitive formation of a presumed **T** species. The **T** species is known to form preferentially with ligands possessing limited steric demands. Ostensibly minor changes, such as the substitution of one ethyl for one methyl substituent in a PDL, is sufficient to change from predominant **O** to predominant **T** formation at parity of other conditions. High initial copper concentrations (> 10 mM) are also known to favor the formation of **T** species.²⁹ The preferential formation of a **T** species are consistent with a pathway that involves a 2:1 Cu(I):O₂ species (an **O** or isomeric side-on peroxo species) as detailed in Scheme 2. The limited steric demands of the ligand are needed to accommodate the compact trinuclear [Cu₃(μ₃-O)₂]³⁺ core and the high concentrations of Cu(I) are needed to rapidly trap the 2:1 species rather than allowing completely forming an **O** species. Trimerization can be suppressed by ligands with greater steric demands allowing exclusive formation of an **O** species. The facile formation of the **T** species with [(TMED)Cu(I)]¹⁺ suggests a susceptible

Cu₂O₂ core that motivates trapping this **O** species and exploring its reactivity with other exogenous substrates.

Despite the dominance of the **T** species with TMED under most circumstances, the **O** species can be stabilized kinetically by inhibiting its subsequent reaction with intact Cu(I) complexes. By optimizing experimental conditions, the **O** species is made observable only in acetone combined with low initial concentrations of Cu (≤ 2 mM). The concentration dependent oxygenation is similar to that of small PDLs such as TMCD²⁹ and MEED,¹² which yield **O** species at low Cu concentrations and **T** species at high concentrations. The concentration dependence can be explained with the postulated oxygenation mechanism in Scheme 2. At high Cu(I) concentrations (> 10 mM), $[(L)Cu(I)]^{1+}$ is in excess of the dissolved O₂ concentration allowing for the bimolecular reaction of $[(L)Cu(I)]^{1+}$ with an **O** species to form a **T** species to be competitive with the oxygenation reaction to form the **O** species. At low Cu(I) concentrations relative to dissolved O₂, the oxygenation reaction to form an **O** species is much faster allowing its complete formation as the kinetic product. Critical to this analysis is the fact that the dissociation reaction of O₂ from an **O** species formed with a PDL is effectively non-existent. Acetone has a high O₂ solubility³⁹ relative to CH₂Cl₂ and THF thereby favoring the formation of **O** species at parity of Cu(I) concentration.

Spectral Properties

The nature of **O** species with TMED is confirmed by UV-Vis spectroscopy, resonance Raman and XAS studies. In the UV-Vis spectra, the 392 nm band with an extinction coefficient of 18.5 mM⁻¹ cm⁻¹ per dimer is characteristic of an **O** species. The band is blue-shifted compared to other PDL **O** species, the features of which are typically observed between 398 nm to 450 nm.¹ The 607 cm⁻¹ band in rRaman spectra, shifted 27 cm⁻¹ upon ¹⁸O₂ substitution, is attributed to the breathing mode of the Cu₂O₂ core.³¹ The unusually intense Cu–N stretching mode at 514 cm⁻¹ and the combination of Cu₂O₂ breathing mode and Cu–N mode at 1127 cm⁻¹ indicates that the excitation into the oxo to Cu(III) CT transition results in significant Cu–N distortions. The 1s → 3d transition of Cu in the pre-edge of XAS spectra is located at 8980.3 eV, consistent with the Cu(III) oxidation state.³² The short Cu...Cu and Cu–O distances obtained from the EXAFS fit also agree the characteristics of a typical **O** species.

Thermal Stability

At a given temperature, the **O** species with TMED is thermally more stable than almost all other **O** species created with PDLs. The decomposition rate (4.8×10^{-4} s⁻¹) is more than 10-fold slower than that measured for the perethylated ligand TEED (7.0×10^{-3} s⁻¹) at identical experimental conditions (263 K, acetone, [Cu] = 1 mM, CF₃SO₃⁻). The improved thermal stability is consistent with the higher activation enthalpy and entropy derived from the Eyring analyses^{17,28} (TMED: $\Delta H^\ddagger = 15(1)$ kcal mol⁻¹, $\Delta S^\ddagger = -15(2)$ cal K⁻¹ mol⁻¹; TEED: $\Delta H^\ddagger = 14(1)$ kcal mol⁻¹, $\Delta S^\ddagger = -13(1)$ cal K⁻¹ mol⁻¹). Further analysis of the thermal decomposition products reveals 25% of the ligand is de-methylated to form *N,N,N'*-trimethylethylenediamine, which indicates that TMED undergoes N–CH₃ hydroxylation at a 50% yield assuming a 2e⁻ oxidation by the **O** species.

Ligand hydroxylation is observed frequently in the thermal decomposition of **O** species,^{2,16,17,40} during which a C–H bond of the ligand is oxygenated by the Cu₂O₂ core (Scheme 3). The ligand C–H hydroxylation is assumed generally to proceed through a hydrogen atom abstraction mechanism as the proton and electron derive from the same C–H bond. From previous deuterium KIE studies,^{16,17} the C–H cleavage is the rate limiting step and therefore variations in the C–H bond dissociation energy (BDE) will differentiate the thermostability

of the **O** species when the rest of ligand properties remains the same. The C–H BDE of a methyl group of TMED is estimated ~ 2 kcal mol⁻¹ higher than that of the ethyl group of TEED,⁴¹ therefore given the same ethylenediamine backbone, the TMED **O** species should be the thermally most stable **O** species in the ED series.

Reactivity with Exogenous Substrates

2,4-Di-*tert*-butylphenol and benzyl alcohol are chosen as representative substrates for reactivity studies of the **O** species. The phenol is coupled to the bis-phenol by many **O** species, including ones with very sterically demanding diamines. The generality of this reaction is consistent with a stepwise ET-PT mechanism as proposed by Itoh *et al.*³³ The small reported KIE (1.21~1.56) associated with O–H(D) cleavage of phenol by an **O** species is a lower bound of known PCETs, leading to the postulation that the single electron transfer from the phenol may be the first and rate-limiting step. As an ET can occur by an outer-sphere mechanism, the phenolic substrate does not need to directly access the **O** core. Therefore most **O** species including both bulky and compact ones should be capable of phenol oxidation.

The limited steric demands of the TMED ligand open the possibility of direct substrate access to the Cu₂O₂ core and an inner-sphere oxidation pathway. The TMED **O** species oxidizes benzyl alcohol to benzaldehyde without the aid of any deprotonation reagent, which is not observed with any other **O** species formed with PDLs.⁴² Isotope studies provide valuable insights into the mechanism. The KIE (O–H/O–D) value of *ca.* 1 suggests that the cleavage of the O–H bond is essentially not involved in the rate limiting step. The KIE values of *ca.* 3, determined both from independent absolute rate kinetic measurements and from intra- and intermolecular competitive reactions, suggest that the C–H bond cleavage is both the rate and product determining step. The KIE in this study is comparable to those reported for hydrogen atom transfer reaction on substrates with benzylic and aliphatic C–H bonds by high-valent metal-oxo species.^{43–45} If the benzyl alcohol oxidation by the **O** species follows a similar mechanism, an exposed **O** core is critical to allow the formation of an O (... H (... C transition state.

4. Conclusion

The current study presents an experimental and theoretical investigation of the simplest of the bis(μ -oxo)dicopper(III) (**O**) species stabilized by the TMED ligand, with the intention of assessing the oxidizing ability of an accessible **O** core to exogenous substrates. Unlike most other PDLs, the oxygenation chemistry of the cuprous complex of TMED is complicated as a dimeric **O** species or a trimeric **T** species can be formed. Low concentration of [(TMED)Cu(I)]¹⁺ relative to the O₂ concentration in acetone with weakly coordinating counter-anions leads to preferential formation of the **O** species, the kinetic product. This dimeric species has been spectroscopically characterized by UV-Vis, rRaman and XAS, and these spectral and metrical features correlate closely with DFT calculations. The enhanced thermal stability of this species presumably results from the higher C–H bond dissociation energy of methyl groups, thereby slowing the intramolecular ligand hydroxylation as a decomposition pathway. The more exposed and accessible core of this **O** species correlates with an enhanced oxidative capacity as it cleanly oxidizes benzyl alcohol, which has not been observed previously for such Cu/O₂ species.

5. Experimental Section

Materials and Methods

All the chemicals were purchased from commercial sources if not mentioned otherwise. CH₂Cl₂, THF and MeCN were of HPLC grade and further purified by the Pure-Solv 400

solvent purification system (Innovative Technology), HPLC grade acetone was distilled under a N₂ atmosphere after refluxing for 5 hrs over K₂CO₃. [Cu(MeCN)₄]X⁻ (X⁻ = CF₃SO₃⁻ or SbF₆⁻) was synthesized from Cu₂O (Aldrich) and trifluoromethanesulfonate acid (Aldrich) or hexafluoroantimonic acid (Aldrich) by a variation of the literature method. ⁴⁶ N,N,N',N'-tetramethylethylenediamine (TMED) was purchased from Aldrich and distilled from CaH₂ under a N₂ atmosphere. Ferrocene monocarboxylic acid (FcCOOH) (Aldrich, 97%) was purified by sublimation in vacuum. Preparation and manipulation of air-sensitive materials were carried out in a N₂ drybox (M. Braun, 1 ppm in O₂ and H₂O). Low-temperature UV-Vis spectra were collected on a Varian Cary 50 Bio spectrophotometer with a custom-designed quartz fiber-optic dip-probe (Hellma) of variable optical pathlength (0.10 or 1.0 cm) in custom-designed sample cells (ChemGlass).

Synthesis and Oxygenation of [(TMED)Cu(I)]¹⁺ Complex

Under an inert atmosphere, equimolar amounts (0.100 mmol each) of [Cu(MeCN)₄] (CF₃SO₃) and TMED were mixed in 5 mL of CH₂Cl₂ to yield a clear, colorless solution. This solution was used immediately after preparation. In a typical oxygenation reaction, 250 μL of freshly prepared Cu(I) solution was injected into 5 mL of acetone saturated with O₂ (1 atm) under vigorous stirring at 183 K, yielding a solution of *ca.* 0.5 mM [Cu₂O₂(TMED)₂]²⁺. If oxygenation occurs at higher copper concentrations ([Cu] > 10 mM), the [(TMED)Cu(I)]¹⁺ solution was first injected into chilled acetone under N₂ followed by purging the head space of the reaction vessel with O₂, yielding a solution of dominantly [Cu(III)Cu(II)₂O₂(TMED)₃]³⁺. Oxygenation in THF and CH₂Cl₂ followed the same procedure as above.

Resonance Raman

Resonance Raman spectra were obtained using a Princeton Instruments ST-135 back-illuminated CCD detector on a Spex 1877 CP triple monochromator with a 2400 grooves/mm holographic spectrograph grating. A laser excitation line of 413.1 nm (provided by a Coherent I90C-K Kr⁺ ion laser) was chosen to enhance and probe the copper-oxygen modes. Spectral resolution was < 2 cm⁻¹. Sample spectra were collected at 77 K with a liquid N₂-filled finger Dewar. The O species with 2 mM in Cu was oxygenated in acetone in an NMR tube and kept frozen in liquid N₂. Isotopic substitution was achieved by oxygenation with ¹⁸O₂ (Icon, 99%).

X-ray Absorption Spectroscopy

O species suitable for X-ray absorption spectroscopy (XAS) were oxygenated in acetone (1 mM in Cu, 5% CH₂Cl₂), and a ~200 μL of sample solution was transferred into a Lucite XAS cell with 37 μm Kapton tape windows and then frozen in liquid N₂. The X-ray absorption spectra were recorded at the Stanford Synchrotron Radiation Lightsource (SSRL) on focused 16-pole wiggler beam line 9-3 with the ring operating at 3 GeV, 80-100 mA. A Si(220) double-crystal monochromator was used for energy selection at the Cu K edge, and a Rh-coated mirror upstream of the monochromator was used for harmonic rejection, and a Rh-coated post-monochromator mirror for vertical and horizontal focusing. The samples were maintained at 10 K during data collection by using an Oxford Instruments CF1208 continuous-flow liquid-helium cryostat. Data were measured in fluorescence mode as Cu Kα fluorescence with a Canberra (Meriden, CT) 30-element solid state Ge array detector. The internal energy calibration was performed by simultaneous measurement of the absorption of Cu foil placed between two ionization chambers filled with N₂ located after the sample. The first inflection point of the foil was assigned to 8980.3 eV. A gradual decrease in the energy of the edge region and slight changes in the EXAFS were observed upon continuous scanning at the same spot. Hence, five distinct and physically separate spots on the two XAS

samples were exposed, and only two first scans at each spot were used for data analysis, for an average of four scans.

The averaged data were normalized with the program XFIT⁴⁷ by first subtracting a polynomial background absorbance that was fit to the pre-edge region and extended over the post-edge with control points, followed by fitting a three-region polynomial spline of orders 2, 3, and 3 over the post-edge region. The data were normalized to an edge jump of 1.0 between the background and spline curves at 9000.0 eV. Theoretical EXAFS signals $\chi(k)$ were calculated using FEFF (version 7.02)⁴⁸ and fit to the nonfiltered data by EXAFSPAK (G.N. George, SSRL). The experimental energy threshold, E_0 , the point at which the photoelectron wavevector $k = 0$, was chosen as 9000.0 eV and was varied in each fit as a common value for every component in the fit. The amplitude reduction factor, S_0^2 , was set to 1.0. The structural parameters that were varied during the refinements included the bond distance (R) and the bond variance (σ^2). Atom types and coordination numbers were systematically varied during the course of the analysis, but were not allowed to vary within a given fit. Data were fitted over the k range of 2–13 Å⁻¹. Fourier transforms of the EXAFS data and second derivatives of the normalized absorption data were calculated with EXAFSPAK.

Thermal Decomposition Kinetics

Upon the complete oxygenation of **O**(TfO)₂ species in acetone solution of 1 mM in Cu, excess O₂ was removed by purging with N₂ for 15 min, and the **O**(TfO)₂ species was allowed to warm and decompose at specific temperatures (256–279 K), which were maintained by a thermostatic cooling bath (Kinetic systems, New York). The temperature of the sample was measured by immersing a thermocouple (Omega) into the solution. Data collection started only after the solution achieved the desired temperature, which required approximately 2–3 min. Multiwavelength (330–600 nm) component analyses of spectral data were performed with SPECFIT⁴⁹ software to obtain the decomposition rate constants. The number of significant eigenvectors obtained was two for all data sets, and a first-order kinetic (A→B) model provided good fits to these data sets.

Thermal Decomposition Product Analysis

O solution (1 mM in Cu, 5 mL acetone, TfO⁻) was prepared at 193 K with excess O₂ removed, and the solution was maintained at 243 K until the 392 nm band completely disappeared. Aliquots of NH₃ aqueous solution (30%) were added to the decomposed reaction product with vigorous shaking, and benzonitrile was added as an internal standard. The solution was dried over K₂CO₃ and passed through neutral activated alumina (Brockmann I, ~150 mesh, 58 Å). The column was washed by 2 ml MeOH. The combined eluent was examined by GC and GC-MS analysis.

Syntheses of Deuterated Benzyl Alcohols—The synthesis of benzyl alcohol-*d* followed the reported procedure in the literature.¹⁹ 1.0 g benzyl alcohol was dissolved in THF and 0.25 g NaH (1.1 equiv) was added. After H₂ evolution ceased, the solution was filtered and D₂O was added to the filtrate. The organic phase was separated and the aqueous phase was extracted with diethyl ether. The combined organic phase was dried over K₂CO₃, and the solvent was removed in vacuo to obtain benzyl alcohol-*d* (95% D by ¹H-NMR).

Syntheses of benzyl alcohol-*α-d*₁ and benzyl alcohol-*α,α-d*₂ also followed the reported procedure in the literature.³⁴

Oxidation of Exogenous Substrates: **O** solution (1 mM in Cu, 5 mL acetone, TfO⁻) was prepared at 193 K with excess O₂ removed. Two equivalents of substrates (benzyl alcohol,

1-octanol or 2,4-di-*tert*-butylphenol) were added to these solutions. The reaction mixture was stirred at 243 K until the distinct **O** feature disappeared. For alcoholic substrates workup, aliquots of 30% NH₃ aqueous solution were added to the reaction mixture. Acetophenone was added as an internal GC standard. The mixture was dried over Na₂SO₄ and passed through neutral activated alumina (Brockmann I, ~150 mesh, 58 Å). The column was washed with 2 ml methanol, and the combined eluent was examined by GC and GC-MS analyses. For phenolic substrates workup, a 10% H₂SO₄ aqueous solution (0.5 mL) was added into the cold reaction mixture before warmed to RT. The organic phase was extracted with CH₂Cl₂, dried over Na₂SO₄ and the solvent was removed under vacuum. The residue was examined by ¹H-NMR (CDCl₃, 300 MHz). The product distribution was calculated by evaluating the signals of the *tert*-butyl groups in each product: 2,4-di-*tert*-butylphenol: 1.42 ppm + 1.29 ppm; 3,3',5,5'-tetra-*tert*-butyl-2,2'-bisphenol: 1.45 ppm + 1.32 ppm.

Rate Measurement of Alcohol Oxidation: 20 equivalents of substrate (PhCH₂OH, PhCH₂OD or PhCD₂OH) were added to an **O** solution (1 mM in Cu, 5 mL acetone, TfO⁻) with excess O₂ removed. The reaction mixture was maintained at 243 K and the decomposition of the **O** species was followed by UV-Vis spectroscopy. Multiwavelength (330–600 nm) component analyses of spectral data were performed with SPECFIT⁴⁹ software to obtain the reaction rate constants. The number of significant eigenvectors obtained was two for all data sets, and a pseudo first-order kinetic (A→B) model provided good fits for these data sets.

Measurement of Intramolecular and Intermolecular Competition KIEs: 2 equivalents of substrates (PhCHDOH for the intramolecular KIE, a 1:1 mixture of PhCH₂OH and PhCD₂OH for the intermolecular KIE) were added into the **O** solutions (1 mM in Cu, 5 mL acetone, TfO⁻) at 243 K. The reactions were carried out following the same procedure as described above. The organic product distribution was analyzed by GC-MS. The overall pattern of *m/z* 105–108 peaks in the mass spectrum of *h*- and *d*-benzaldehyde was fitted by a linear combination of individual patterns of *h*- and *d*-benzaldehyde.

Computational Details—Density functional theory (DFT) calculations were performed using a Gaussian 03 program⁵⁰ (revision C.02) on a Linux cluster. The unrestricted wave function was used for the singlet ground state of [(TMED)₂Cu₂O₂]²⁺. The functionals are pure functional BLYP^{51,52}, hybrid functionals B3LYP⁵³ and BHandHLYP (as implemented in Gaussian 03) with 20% and 50% of HF exchange respectively. Basis Set 1 (BS1) uses a triple- ζ 6-311+G(d) basis set on Cu, O and N atoms and a double- ζ 6-31G(d) basis set on C and H atoms.

The geometry optimizations were performed using the above three functionals with BS1 or 6-31G(d) basis set, followed by frequency calculations on each optimized structure with corresponding functional/basis set. Time-dependent density functional theory⁵⁴ (TD-DFT) calculations were performed using the above functionals and basis sets on the geometry optimized by the vacuum B3LYP/6-31G(d) method. The polarized continuum model⁵⁵ (PCM) was used in the TD-DFT calculations to model the solvation environment in acetone (dielectric $\epsilon = 20.7$) with a United Atom (UA0) radii scheme. UV-Vis spectra were simulated using the SWizard⁵⁶ program with a Gaussian model and the half-bandwidth of 2500 cm⁻¹. Mulliken population analysis of molecular orbitals was calculated using the AOMix program.⁵⁷

Supplementary Material

Refer to Web version on PubMed Central for supplementary material.

Acknowledgments

Funding was provided by the NIH GM50730 (T.D.P.S.), NIH DK31450 (E.I.S.) and NIH RR-01209 (K.O.H.). XAS data were measured at SSRL that is supported by the Department of Energy, Office of Basic Energy Sciences. The Structural Molecular Biology program at SSRL is funded by the National Institutes of Health, National Center for Research Resources, Biomedical Technology Program, and the Department of Energy, Office of Biological and Environmental Research. This publication was made possible by Grant Number 5 P41 RR001209 from the National Center for Research Resources (NCRR), a component of the National Institutes of Health (NIH). Its contents are solely the responsibility of the authors and do not necessarily represent the official view of NCRR or NIH.

References

1. Mirica LM, Ottenwaelder X, Stack TDP. *Chem Rev.* 2004; 104:1013–1045. [PubMed: 14871148]
2. Lewis EA, Tolman WB. *Chem Rev.* 2004; 104:1047–1076. [PubMed: 14871149]
3. Karlin, KD.; Tyeklár, Z. *Bioinorganic Chemistry of Copper.* Chapman & Hall; New York: 1993.
4. Schindler S. *Eur J Inorg Chem.* 2000; 2311–2326
5. Itoh S, Tachi Y. *Dalton Trans.* 2006:4531–4538. [PubMed: 17016563]
6. Halfen JA, Mahapatra S, Wilkinson EC, Kaderli S, Young VG, Que L, Zuberbuhler AD, Tolman WB. *Science.* 1996; 271:1397–1400. [PubMed: 8596910]
7. Obias HV, Lin Y, Murthy NN, Pidcock E, Solomon EI, Ralle M, Blackburn NJ, Neuhold YM, Zuberbuhler AD, Karlin KD. *J Am Chem Soc.* 1998; 120:12960–12961.
8. Mahadevan V, Henson MJ, Solomon EI, Stack TDP. *J Am Chem Soc.* 2000; 122:10249–10250.
9. Solomon EI, Sundaram UM, Machonkin TE. *Chem Rev.* 1996; 96:2563–2605. [PubMed: 11848837]
10. Mirica LM, Vance M, Rudd DJ, Hedman B, Hodgson KO, Solomon EI, Stack TDP. *Science.* 2005; 308:1890–1892. [PubMed: 15976297]
11. Tolman WB. *Acc Chem Res.* 1997; 30:227–237.
12. Stack TDP. *Dalton Trans.* 2003:1881–1889.
13. Hayashi H, Fujinami S, Nagatomo S, Ogo S, Suzuki M, Uehara A, Watanabe Y, Kitagawa T. *J Am Chem Soc.* 2000; 122:2124–2125.
14. Spencer DJE, Aboeella NW, Reynolds AM, Holland PL, Tolman WB. *J Am Chem Soc.* 2002; 124:2108–2109. [PubMed: 11878952]
15. Herres-Pawlis S, Verma P, Haase R, Kang P, Lyons CT, Wasinger EC, Florke U, Henkel G, Stack TDP. *J Am Chem Soc.* 2009; 131:1154–1169. [PubMed: 19119846]
16. Mahapatra S, Halfen JA, Tolman WB. *J Am Chem Soc.* 1996; 118:11575–11586.
17. Cole AP, Mahadevan V, Mirica LM, Ottenwaelder X, Stack TDP. *Inorg Chem.* 2005; 44:7345–7364. [PubMed: 16212361]
18. Mirica LM, Vance M, Rudd DJ, Hedman B, Hodgson KO, Solomon EI, Stack TDP. *J Am Chem Soc.* 2002; 124:9332–9333. [PubMed: 12167002]
19. Mahadevan V, DuBois JL, Hedman B, Hodgson KO, Stack TDP. *J Am Chem Soc.* 1999; 121:5583–5584.
20. Ottenwaelder X, Rudd DJ, Corbett MC, Hodgson KO, Hedman B, Stack TDP. *J Am Chem Soc.* 2006; 128:9268–9269. [PubMed: 16848427]
21. Mahadevan V, Hou ZG, Cole AP, Root DE, Lal TK, Solomon EI, Stack TDP. *J Am Chem Soc.* 1997; 119:11996–11997.
22. Caulton KG, Davies G, Holt EM. *Polyhedron.* 1990; 9:2319–2351.
23. Mijs, WJ.; Jonge, CRHId. *Organic Syntheses by Oxidation with Metal Compounds.* Plenum Press; New York: 1986. p. 423
24. Paquette, LA. *Encyclopedia of Reagents for Organic Synthesis.* Vol. 2. John Wiley and Sons; New York: 1988. p. 1333-1336.
25. Hay AS, Blanchard HS, Endres GF, Eustance JW. *J Am Chem Soc.* 1959; 81:6335–6336.
26. Hay AS. *J Org Chem.* 1962; 27:3320–3321.
27. York JT, Brown EC, Tolman WB. *Angew Chem Int Ed.* 2005; 44:7745–7748.

28. See the Supporting Information.
29. Cole AP, Root DE, Mukherjee P, Solomon EI, Stack TDP. *Science*. 1996; 273:1848–1850. [PubMed: 8791587]
30. Taki M, Teramae S, Nagatomo S, Tachi Y, Kitagawa T, Itoh S, Fukuzumi S. *J Am Chem Soc*. 2002; 124:6367–6377. [PubMed: 12033867]
31. Henson MJ, Mukherjee P, Root DE, Stack TDP, Solomon EI. *J Am Chem Soc*. 1999; 121:10332–10345.
32. DuBois JL, Mukherjee P, Stack TDP, Hedman B, Solomon EI, Hodgson KO. *J Am Chem Soc*. 2000; 122:5775–5787.
33. Osako T, Ohkubo K, Taki M, Tachi Y, Fukuzumi S, Itoh S. *J Am Chem Soc*. 2003; 125:11027–11033. [PubMed: 12952484]
34. Pratt RC, Stack TDP. *Inorg Chem*. 2005; 44:2367–2375. [PubMed: 15792472]
35. The hybrid functional B3LYP tends to over-stabilize the ⁵P isomer compared with the pure functional BLYP. See: Lewin JL, Heppner DE, Cramer CJ. *J Biol Inorg Chem*. 2007; 12:1221–1234. [PubMed: 17710449]
36. The scale factor for the frequency calculations at B3LYP/6-31G(d) is 0952 See: Alecu IM, Zheng J, Zhao Y, Truhlar DG. *J Chem Theory Comput*. 2010; 6:2872–2887.
37. The extinction coefficient is corrected from the experimental value assuming an 80% formation of TMED O species by FcCOOH titration.
38. Pasquali M, Floriani C, Venturi G, Gaetanimanfredotti A, Chiesivilla A. *J Am Chem Soc*. 1982; 104:4092–4099.
39. Battino, R. IUPAC Solubility Data Series, Oxygen and Ozone. 1. Pergamon; Oxford; New York: 1981. p. 7
40. Itoh S, Taki M, Nakao H, Holland PL, Tolman WB, Que L, Fukuzumi S. *Angew Chem Int Ed*. 2000; 39:398–400.
41. Wayner DDM, Clark KB, Rauk A, Yu D, Armstrong DA. *J Am Chem Soc*. 1997; 119:8925–8932.
42. O species of *N,N,N',N'*-tetramethyl-1,3-propanediamine (TMPD) reported by Stack, et al. (*J Am Chem Soc*. 1999; 121:5583.) can oxidize benzyl alcohol to benzaldehyde in the presence of triethylamine, however, no significant KIE of O-H(D) or C-H(D) is observed, suggesting a different oxidation mechanism from TMED O species.
43. Mayer JM. *Acc Chem Res*. 1998; 31:441–450.
44. Gardner KA, Mayer JM. *Science*. 1995; 269:1849–1851. [PubMed: 7569922]
45. Bell SR, Groves JT. *J Am Chem Soc*. 2009; 131:9640–9641. [PubMed: 19552441]
46. Kubas GJ, Monzyk B, Crumbliss AL. *Inorg Synth*. 1979; 19:90–92.
47. Ellis PJ, Freeman HC. *J Synchrotron Radiat*. 1995; 2:190–195.
48. Ankudinov AL, Rehr JJ. *Phys Rev B*. 1997; 56:R1712–R1715.
49. Binstead, RA. SPECFIT. Spectrum Software Associates; Chapel Hill, NC: 1996.
50. Frisch, MJ., et al. Gaussian 03, Revision C.02. Gaussian, Inc; Wallingford, CT: 2004.
51. Becke AD. *Phys Rev A*. 1988; 38:3098–3100. [PubMed: 9900728]
52. Lee CT, Yang WT, Parr RG. *Phys Rev B*. 1988; 37:785–789.
53. Becke AD. *J Chem Phys*. 1993; 98:5648–5652.
54. Stratmann RE, Scuseria GE, Frisch MJ. *J Chem Phys*. 1998; 109:8218–8224.
55. Barone V, Cossi M, Tomasi J. *J Comput Chem*. 1998; 19:404–417.
56. Gorelsky, SI. SWizard program. University of Ottawa; Ottawa, Canada: 2009. <http://www.sg-chem.net/>
57. Gorelsky, SI. AOMix: Program for Molecular Orbital Analysis. University of Ottawa; 2009. <http://www.sg-chem.net/>

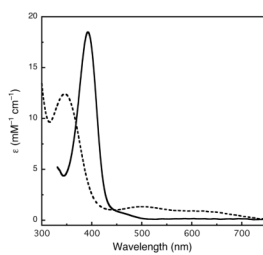


Figure 1. UV-Vis spectra of the TMED **O** species (solid, [Cu] = 1 mM, CF_3SO_3^- , acetone) and proposed TMED **T** species (dash, [Cu] = 1 mM, CF_3SO_3^- , THF) at 183 K.

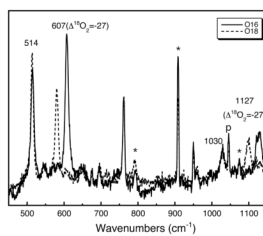


Figure 2. Resonance Raman spectra of $[(\text{TMED})_2\text{Cu}(\text{III})_2\text{O}_2](\text{CF}_3\text{SO}_3)_2$ species ($\lambda_{\text{ex}}=413.1$ nm, 10% $\text{CH}_2\text{Cl}_2/90\%$ acetone, 77 K, $[\text{Cu}] = 2$ mM) oxygenated with $^{16}\text{O}_2$ (solid line) or $^{18}\text{O}_2$ (dash line). Solvent peaks are labeled with an * mark, plasma line is labeled with a “p”.

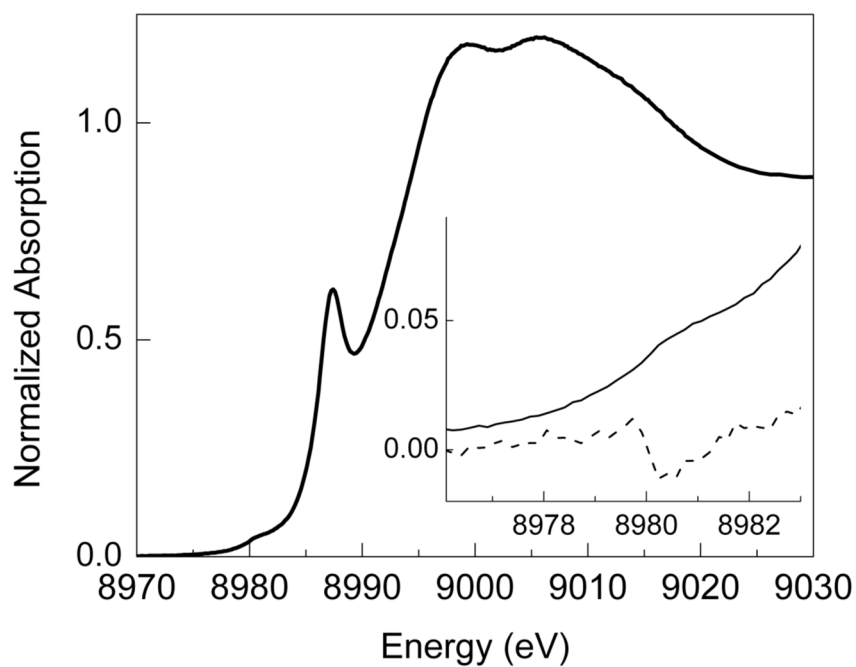


Figure 3. Normalized Cu K-edge absorption spectrum of $[(\text{TMED})_2\text{Cu}(\text{III})_2\text{O}_2](\text{SbF}_6)_2$ in acetone (5% CH_2Cl_2 , $[\text{Cu}] = 1 \text{ mM}$, 10 K). The inset shows the magnified pre-edge region (solid) and its smoothed second derivative (dashed).

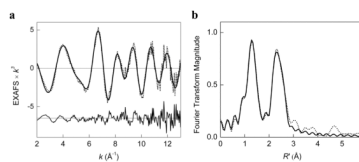


Figure 4.

(a) Cu K-edge k^3 -weighted EXAFS data for $[(\text{TMED})_2\text{Cu}(\text{III})_2\text{O}_2](\text{SbF}_6)_2$ (top) with offset fit residual (bottom) and (b) corresponding non-phase shift corrected Fourier transforms. Data (.....); fit (—).

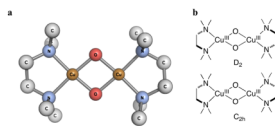


Figure 5. (a) DFT optimized D_2 geometry of $[(\text{TMED})_2\text{Cu}(\text{III})_2\text{O}_2]^{2+}$ with B3LYP/6-31G(d) method (Hydrogen atoms are omitted for clarity): Cu-O = 1.79 Å, Cu-N = 1.95 Å, Cu(\cdots)Cu = 2.72 Å, O(\cdots)O = 2.31 Å. (b) Scheme of two limiting high-symmetry conformations.

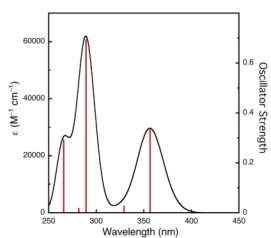
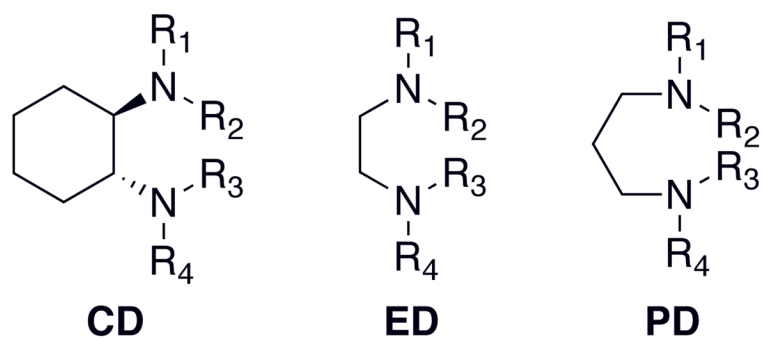
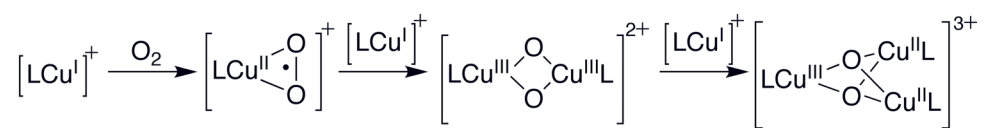


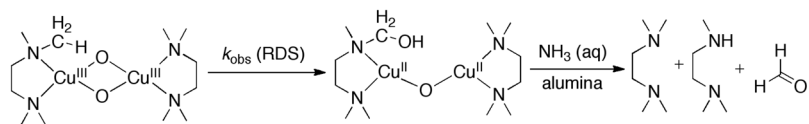
Figure 6. Oscillator strength and simulated electronic spectra of $[(\text{TMED})_2\text{Cu}(\text{III})_2\text{O}_2]^{2+}$ from DFT calculation with PCM-TD-B3LYP/BS1//B3LYP/6-31G(d) method (half-bandwidth = 2500 cm^{-1}).



Scheme 1.
Peralkylated diamine ligands (PDLs).

**Scheme 2.**

Proposed mechanism for formation of **O** and **T** species (L = ligand).

**Scheme 3.**

Proposed N-dealkylation decomposition mechanism of $[(\text{TMED})_2\text{Cu}(\text{III})_2\text{O}_2]^{2+}$ species.

Table 1

Kinetic isotope effects in the oxidation of deuterated benzyl alcohols

| Substrates | PhCH ₂ OH/PhCD ₂ OH ^a | PhCHDOH ^b | PhCH ₂ OH + PhCD ₂ OH ^c | PhCH ₂ OH/PhCH ₂ OD ^a |
|------------|--|----------------------|--|--|
| KIE | 3.3(4) | 2.8(1) | 3.5(2) | 1.12(7) |

^a k_H/k_D from independent kinetic measurements by UV-Vis (20 eq. alcohol, averaged from three measurements).

^b The PhCDO/PhCHO ratio in the reaction product.

^c The PhCHO/PhCDO ratio in the reaction product.

Table 2Metrical parameters optimized by different DFT methods for [(TMED)₂Cu(III)₂O₂]²⁺.

| Functional/Basis Set | Cu...Cu (Å) | O...O (Å) | Cu-O (Å) | Cu-N (Å) |
|----------------------------|-------------|-----------|----------|----------|
| BLYP/6-31G(d) | 2.77 | 2.33 | 1.81 | 1.97 |
| B3LYP/6-31G(d) | 2.72 | 2.31 | 1.79 | 1.95 |
| BHandHLYP/6-31G (d) | 2.66 | 2.30 | 1.76 | 1.94 |
| BLYP/BS1 ^a | 2.82 | 2.37 | 1.84 | 2.02 |
| B3LYP/BS1 ^a | 2.76 | 2.34 | 1.81 | 1.99 |
| BHandHLYP/BS1 ^a | 2.69 | 2.32 | 1.77 | 1.96 |
| Experiment (EXAFS) | 2.74 | – | 1.80 | 1.96 |

^aBS1 uses a 6-311+G(d) basis set on Cu, O and N atoms and a 6-31G(d) basis set on C and H atoms.

Table 3

Selected experimental resonance Raman and calculated Raman vibration modes (B3LYP/6-31G(d)) for [(TMED)₂Cu(III)₂O₂]²⁺.

| Normal Mode (¹⁸ O isotope downshift) | Experimental (cm ⁻¹) | DFT (cm ⁻¹) |
|--|----------------------------------|-------------------------|
| Cu ₂ O ₂ breathing | 607 (27) | 679 (32) |
| Cu-N | 514 (0) | 541 (1) |
| Cu ₂ O ₂ flexing | - | 141 (0) |

Table 4

Experimental and calculated absorption spectra (TD-DFT) on the D_2 symmetric geometry $[(\text{TMED})_2\text{Cu}(\text{III})_2\text{O}_2]^{2+}$ optimized at B3LYP/6-31G(d) level.

| Functional/Basis set | Energy (nm) | Oscillator Strength | Energy (nm) | Oscillator Strength |
|------------------------|-------------|---------------------|-------------|---------------------|
| Experiment | 392 | 0.23 | - | - |
| <i>Vacuum</i> | | | | |
| BLYP/6-31G(d) | 375 | 0.12 | 301 | 0.63 |
| B3LYP/6-31G(d) | 338 | 0.28 | 274 | 0.63 |
| BHandHLYP/6-31G(d) | 298 | 0.54 | 234 | 0.56 |
| BLYP/BS1 | 393 | 0.11 | 311 | 0.72 |
| B3LYP/BS1 | 354 | 0.25 | 286 | 0.65 |
| BHandHLYP/BS1 | 311 | 0.54 | 245 | 0.55 |
| <i>PCM^a</i> | | | | |
| BLYP/6-31G(d) | 376 | 0.16 | 305 | 0.67 |
| B3LYP/6-31G(d) | 340 | 0.36 | 276 | 0.67 |
| BHandHLYP/6-31G(d) | 301 | 0.66 | 235 | 0.59 |
| BLYP/BS1 | 393 | 0.15 | 315 | 0.80 |
| B3LYP/BS1 | 357 | 0.34 | 289 | 0.69 |
| BHandHLYP/BS1 | 315 | 0.66 | 246 | 0.57 |

^a Acetone (dielectric $\epsilon = 20.7$) with United Atom Topological Model (UA0) radii.